ENSTA Bretagne
Ifremer
15ÈMES JOURNÉES DE L'HYDRODYNAMIQUE
22 - 24 novembre 2016 - Brest

Experimental study of underwater blast wave attenuation by bubble curtains

Etude expérimentale de l'atténuation d'une onde de souffle sous marine par rideau de bulles

Florina PANĂ[a], Michel ARRIGONI[b], CélibneGABILLET[c], Octavian ORBAN[a]
[a]Mechanical Engineering, Military Technical Academy of Bucharest,050141 Romania
[b]Institut de Recherche Dupuy de Lôme, ENSTA Bretagne, 2 rue François Verny, 29806 Brest, France
[c]*IRENav*. ECOLE NAVALE, BP 600. LanvéocPoulmic 29240 - Brest naval, France

Summary

This paper announces the preliminary results concerning underwater blast wave attenuation. The purpose of the paper is to design a piece of equipment able to generate a bubble curtain in water and to characterize its blast wave mitigation capability. Such equipment can find its application in harbor safety and during mine clearance operations as well as during offshore wind farms installation. Experiments consist of generating dynamic pressure into a water tank by the use of a gas gun. Time resolved pressure records were performed by the use of PVDF shock gauges as hydrophone. Numerical modelling based on finite element method in explicite scheme tends to agree with experiments.

Résumé

Les travaux ci-présentés divulguent les résultats préliminaires concernant l'atténuation d'une onde de choc dans l'eau par la méthode des rideaux de bulles. Le but est de concevoir un dispositif capable de générer un rideau de bulles dans l'eau et d'en caractériser sa capacité d'atténuation des ondes de choc. Un tel dispositif, extrapolé à une plus grande échelle, peut trouver une application dans la sécurité portuaire et lors des opérations de déminage, ainsi que lors de l'installation des parcs éoliens offshores. Les expériences consistent à générer une pression dynamique dans un réservoir d'eau par l'utilisation d'un canon à gaz. Les enregistrements de pression ont été réalisés par l'utilisation de jauges de choc PVDF utilisées en hydrophone. La modélisation numérique basée sur la méthode des éléments finis en schéma explicite fournit des résultats qui se rapprochent de ceux obtenus par l'expérience.

1. Introduction

Underwater explosions generate intense compression waves that can propagate in large distances and cause a threat for structures and sea life.

In the same registry, during farm installation, the use of the pile driving technique (hammer that strikes a pile to plant it on the seabed) generates an important noise pollution because of the compressive waves transmitted into the water. On the one hand, the sound exposure can provoke migration of animal species like marine mammals and thus, devastate the local biotope (Koschinschi et al, 2013). It is accepted that producing clean, safe and efficient energy is one of the major challenges that our society has to cope with. For example, renewable energies such as offshore wind farms are identified as clean and efficient solutions that are being increasingly used along coasts. On the other hand, conscient of this concern, the juridic context is becoming less and less tolerant to the noise pollution introduced by human activities in the oceans and seas. Sound exposure levels generated by human activities are now wanted to be limited by regulations.

An existing solution regarding underwater noise and shock wave mitigation consists on using a biphasic barrer, like bubble screens or curtains. Literature offers vast knowledge when it comes to gas bubble formation and existence in liquid media.

The idea of using air bubbles in water is far from being new since it has been first proposed for blast wave mitigation (Mallock 1910). In 1955, La Prairie has patented the use of bubble curtains as mitigation method for underwater shock waves effects (La Prairie, 1955). Bubble curtain mitigation capacity, regarding shock wave propagation, has been studied more in details considering the normal interaction of a shock wave with a pressure pulse in the form of a semi-infinit step (Surov 1998). A completed description performed in the field of bubble polydispersed flow and its effect over shock wave parameters, has been presented by Ando et. al in 2011. The purpose of his work was to study a continuum bubbly flow that incorporates a distribution of equilibrium bubble nuclei sizes and quantify the effect of polydispersity on averaged shock dynamics.

More recently, Grandjean, has implemented a physical model in a numerical finite element code which characterize the mechanisms that contribute to shock wave attenuation as thermal and viscous effects or heterogeneous gas fraction profiles (bubble clusters) (Grandjean 2012). Hhis model is based on the Rayleigh-Plesset equation completed with heat transfert term, coupled with an equation of state for gas and water and a fission condition. Concerning experimental approaches at laboratory scale, several approaches have been porposed. Kameda used a shock tube ended with a liquid filled section in which monodispersed bubbles were generated (Kameda 1998). His results have been used by Grandjean for the validation of his modelling. Preocupations in the domain of underwater shock wave mitigation have included the research of other attenuation configurations as porous materials, (Saito et al 2003) or sandwich structures having core materials between two face sheets (Espinosa et al 2006). In this last approach, Espinoza used a gas gun for impacting a plate on a liquid filled tank in order to generate a tailored impulse than can match a blast wave temporal profile. Croci proposed a comparable device than can induce a series of mechanical impulses that are between a blast profile and a pile driving (Croci, 2014). He also proposed a bubble curtain generator based on a porous pipe coupled with a digital flowmeter. He could perform a local characterization of the bubble curtain by the use of an optical probe at the laboratory scale. He could then evaluate the peak pressure mitigation procured by the curtain itself. In his experiments, the curtain generated by a porous pipe was not structured, making difficult the observation and the interpretation of the role played by the bubble size and the void fraction. At last, the wavelength of the loading generated in the water was of the order of magnitude of the curtain thickness so the impedance mismatch between the water and the curtain played an important role.

In this work is presented additional experimental results obtained with a similar setup. The purpose of this paper is to design a piece of equipment able to generate a bubble curtain in water and to characterize its compression wave mitigation capability with respect to its air volume fraction in the liquid, its bubble size and its gas flowrate. The design also tackles the matter of dynamic underwater pressure measurement by the use of PVDF technique. The overall process is considered: shock generation and characterization, bubbly media generation and characterization and at last, pressure mitigation. The wavelength of the loading has been chosen larger than the curtain thickness in order to assess the mitigation by the bublle dynamics effects described by Grandjean. It will become a laboratory tool for determining optimal solution for mitigation of underwater noise pollution.

In the first part, a simple bubbling system is presented and characterized. The second part evidences the shock mitigation by bubbly media in two impact conditions. It also shows time resolved pressure measurement by the use of PVDF “Bauer” shock gauges. The third part shows finite element calculations that illustrate the shock propagation occurring during the experiments and correlate the observations.

2. Theoretical study regarding bubble generation through immersed perforated pipes

Gas bubbles in liquid have been studied from the theoretical point of view starting with their formation in constant flow or constant pressure condition and ending with analyze of their dynamics and thermal behavior. Bulson proposed the theory of bubble curtain based on analytical and experimental considerations (Bulson, 1968). However, it has been chosen a simple bubble generator in order to obtain a bubbly media as monodisperse as possible.

Theoretical and experimental approaches considering the influence of viscosity, surface tensions and density of Newtonian liquid on bubble formation can be found in the literature. Ramakrishnan, (Ramakrishnan, 1968) described the bubble formation through a single orifice by a mathematical model. In the same year, Satyanarayan obseved the bubble formation under constant pressure conditions (Satyanarayan, 1968). He described the formation of bubbles during two stages through a single orifice (Ramakrishnan and Satyanarayan, 1968), taking into account the effects of physical properties of the liquid on the bubble size. Their models were consistent only for spherical bubbles that are rather deformed in operational conditions.

Gas bubble deformation in different types of liquids, for Morton number ($M_0 = \mu^4 g / \sigma^3 \rho$) varying between 10^{-11} and 10^0, has been studied recently (Legendre, 2012). In his study, it has been proposed a simple equation for bubble deformation and then compared with results given by (Moor, 1985).

Bubble formation through multiple orifices has been investigated from theoretical and experimental point of view. One of the purposes of the study is to propose a mathematical model able to predict bubbling frequency, bubble radius and gas chamber volume under various conditions (Xie, 2003).

In the presented work, an air bubble curtain was generated by immersed pipes that are regularely spaced perforated (fig. 1), at different flow rates (6 l/min and 7 l/min) and with different pipe configurations. The bubbler parameters were respectively the pipe material (PVC, Al), the holes spacing (10 mm, 12 mm), holes diameter (0.8 mm and 1.2 mm) and number of holes (21 and 14). These parameters allowed us to obtain a variety of controlled bubble curtains that finally were characterized with respec tto their shock wave mitigation capacity.

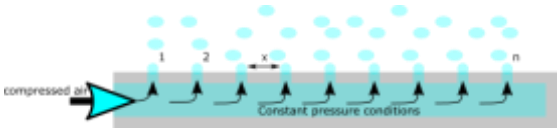

Figure 1.Schematic representation of bubbling system

3. Experimental set-up for bubble curtain characterisation

In the present study, it has been considered that bubbles formation respects the condition of constant pressure inside the pipe. The bubbly media so obtained has been characterized by the use of an optical probe like in (Croci, 2014), correlated with video and acoustic observations in order to determine bubble mean radius.

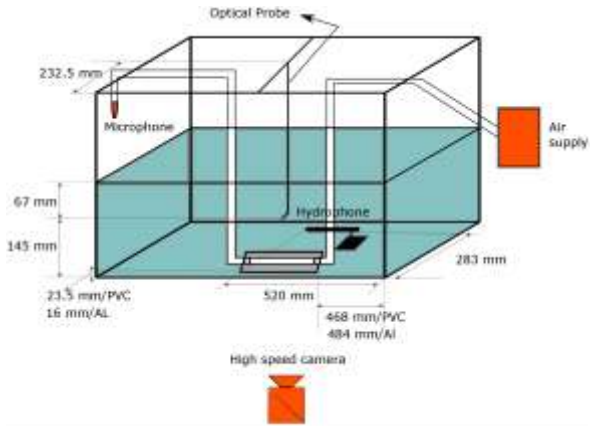

Figure 2.Experimental configuration for bubble curtain characterization

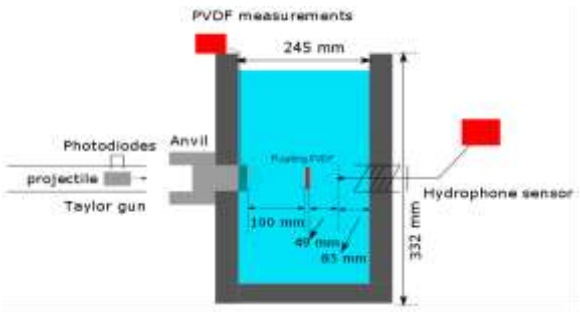

Figure 3.Experimental configuration for tests without bubble curtain

The figure 2 shows an experimental setup with the apparatus used for the bubbler characterization where the flow rate inside the immersed pipe has been controled by a controle valve. Varying the flow rate and pipe configuration, the bubbles formation through the orifices and their flow at a constant immersion depth has been recorded with a high speed camera, Photron® APX, at 1000 images/second during 2 min for both pipes. The other end of the pipes has been connected to a Bruel&Kjer® microphone set at 12.000 mV/Pa, able to record the sonar activity inside the pipe, between 0.1 Hz to 50 kHz generated by bubbling process, and provide a voltage signal to the oscilloscope through a NEXUS® charge amplifier. For a similar purpose, another piece of equipment has been used in the position described by fig. 2, as a third device that monitors acustics inside the water aquarium. The hydrophone signal has been analyzed on an Odyssey data aquisition system after using a NEXUS® charge amplifier with a coefficient of 31.6 mV/Pa and pass band 1 Hz to 22.4 kHz. The transducer has been set at 0.102 pC/Pa according to its data sheet.

4. Experimental set-up for shock wave generation and mitigation in biphasic media

The experimental set-up (fig. 3) consists in a 50 mm diameter Taylor gun shooting aluminium projectile guided by a PMMA sabot at an aluminium anvil inserted into the side wall of a water tank. The diameter of the anvil is 60 mm and its length is 81 mm. The inner dimensions of the water tank are 33 cm large, 24.5 cm long and 20 cm depth. The aluminium projectile is a 40 mm diameter cylinder with a 40 mm lengtht. The terminal velocity is measured by the use of two photodiode barriers.

The underwater shock pressure is recorded by two measuring techniques: with a T11 Sonar Neptune® hydrophone and 25 µm thick PVDF pressure sensors in current mode (Bauer, 2000). The generated underwater pressures are measured with and without bubble curtain. A first PVDF sensor is placed at the water/anvil interface. It provides time resolved pressure records related to stress waves transmitted from the anvil into the water. ThisPVDFsensor was connected to a LeCroy® oscilloscope with a maximum bandwidth of 500 MHz and with an acquisition rate of 1GSamples/s.

A second PVDF sensor is placed in the water, in “floating mount”, at the place of the bubble curtain when it is turned off (fig. 3). This floating PVDF is connected in current mode (50 Ohm) in a Tektronix® oscilloscope having a bandwidth of 350 MHz and a acquisition rate of 1GSamples/s. The hydrophone T11 is also connected to this oscilloscope through a Müller® charge amplifier. Its piezoelectric coefficient is 74 pC/MPa. The hydrophone has given a voltage signal to Tecktronix oscilloscope, characterized by a maximum frequency of 350 MHz and an aquisition frequency 1GS/s.

The bubble curtain ability of reduction of the peak pressure and impulse of the compression wave are considered as its most important characteristics. Two types of pipes for blowing air are immersed into the water perpendicular to the gun axis (fig. 4). The first pipe, noted A, is defined by a PVC material, 21 holes with 0.8 mm diameter and 10 mm in between. The second pipe, noted B, differs from the first by its material, made of Al, 14 holes with hole diameter 1.2 mm and 12 mm between them.

The wave generated by a quasi-planar impact between the projectile and the anvil have some similarities with respect to a blast wave, since it has a sharp compression front and the releases coming from the sides of the anvil result in a gradually drop of pressure. The positive phase of the wave is transmitted from the anvil to the water, whereas the negative phase is likely to cause water cavitation near the anvil, as it was observed by fast video camera.

5. Experimental results

Bubbling frequencies observed for a given configuration are presented in table 1 and figure 5.

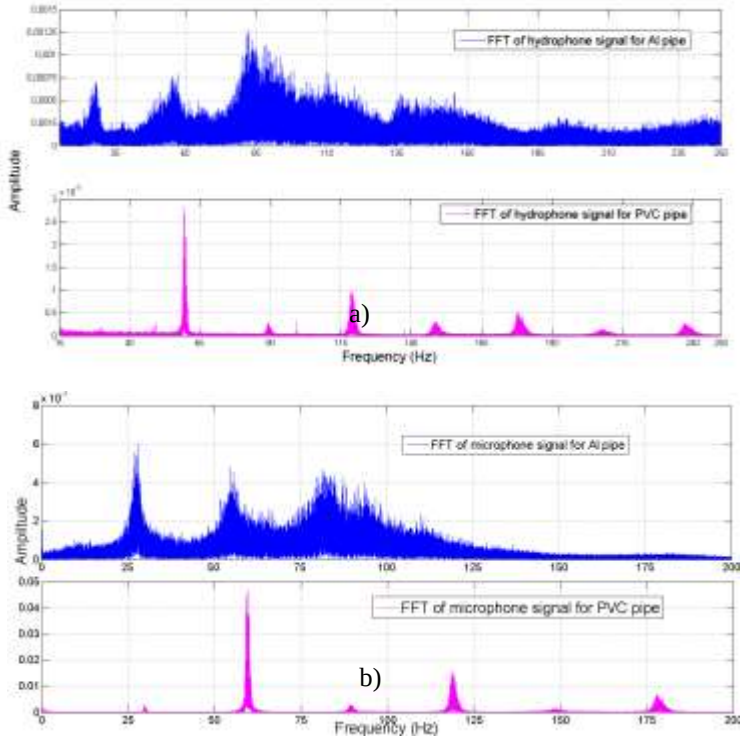

Figure 5.Bubble formation frequency coresponding hydrophone a) and microphone b) for 7 l/min (blue) and 6 l/min (magenta)

Table 1 Bubble formation frequency:

Pipe	Flow rate l/min	Sound sensor	Frequency Hz
A	6	microphone (fig. 5 a)	29.8
		hydrophone (fig. 5 b)	29.67
B	7	microphone (fig. 5 a)	28.06
		hydrophone (fig. 5 b)	27.62

Microphone results, described in fig.5 a), have been compared with hydrophone data given in fig. 5 b), where it has been observed a good correlation between values of the bubble formation frequencies.

Experimental configurations regarding shock wave generation and attenuation are gathered in table 2 giving the impact velocity in m/s, Pmax the maximum pressure in MPa, Is the positive impulse in MPa.ms and the curtain configuration (No, A, B and related flowrate). Impact velocities correspsond to a given compressed air pressure loading of the Taylor gun.Two air compressed loading pressure have been chosen: 2 Bar and 7 Bar (absolute).The resulting impact velocity is not exactly reproducible and may vary in the range of ± 0.015 m/s for a 2 Bar loading and of ± 4 m/s for a 7 Bar loading, depending on experimental conditions (ambiant pressure, sabot adjustment, impact planarity).

Table 2: Shock wave parameters obtained from hydrophone measuremets

Shot #	Terminal velocity m/s	Curtain	Pmax (MPa)	Positive impulse MPa*ms
1	16	off	1.41	0.0133
2	15.7	A (6 l/min)	0.19	0.00134
3	50.7	off	7.02	0.06
4	42	B (7 l/min)	0.76	0.009
5	51.5	A (6 l/min)	1.37	0.01

A: PVC pipe with 21 holes of 0.8 mm diameter, with flowrate of 6 L/min.

B: Al pipe with 14 holes of 1,2 mm diameter, with flowrate 7 l/min.

Experimental data given by PVDF measurements (fig. 6), at the interface between anvil and water, puts in evidence the reproducebility of the trials when the underwater shock wave has been generated at impact velocities aproximatly 16 m/s ± 0.5. Data acquision has been realised by triggering from the amplified PVDF channel, where the charge amplifier has been used in order to convert the charge/MPa into V/MPa and compare the pressure profile with the one given from measurements in direct mode.

The first rising front corresponds to the first compression wave generated by the impact of the projectile onto the anvil. The slope is not perfectly straight due to the no- ideally flat impact. The first large double peak lasts about 15 µs, which is the duration of the loading given by the projectile, as being the back and forth time of the shock and release wave in twice 40 mm with a bulk sound velocity of about 5.38 mm/µs (see table 7). The presence of a double peak in this first peak is explained by the interaction of the reflected waves on the cylindrical lateral side of the anvil (similar to Pochammer-Chree effects (Graff 1975)). The lateral waves also affect the rest of the signal by adding minor inflections. The period of about 40 µs between the two major peaks corresponds to the back and forth in the anvil plus projectile of about 242 mm at 5.38 m/s.

The hydrodynamic pressure transmitted into the water is then estimated to be 7.75 MPa ± 1.25.

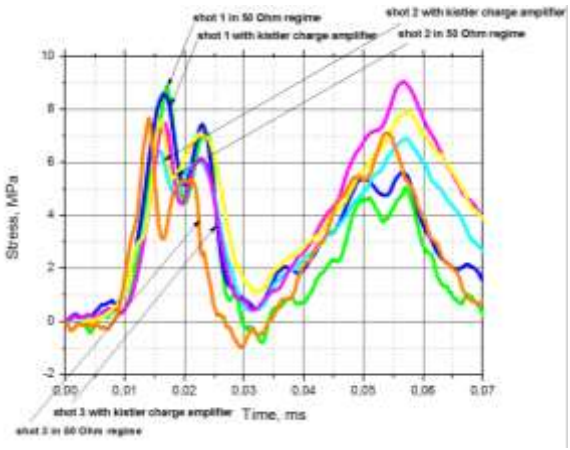

Figure 6.Overpressure resulted from PVDF measuremets at the anvil/water interface

The difference between pressure profiles corespunding to different impact velocities occurs, most probably, due to imperfect planarity involving a different impact angle from a shot to another.

Table 3: Impact velocity for measurements with fixed PVDF

Shot #	Terminal velocity m/s
1	16,51
2	16.59
3	15.53

Table 4: Impact velocity for measurements with floating PVDF and hydrophone

Shot #	Terminal velocity m/s
4	50.69
5	46.79

The same approach was carried out with the floating PVDF (fig. 3), verticalypositioned into the water, with its sensitive area coinciding with the barrel and anvil axis, at 100 mm of the free surface of the anvil. Time resolved pressure measurements are shown on figure 7 a) and b). They are in agreement regarding the chronology but the pressure measured by the hydrophone is about 50 % higher than the one measured by the PVDF. It can be explained by a possible reflection of the pressure wave on the hydrophone holder. This difference is even more pronounced at higher pressure (fig. 7 b)). The time resolved pressure is recorded during

a much longer time than what shown in figure 7, about 10 ms, and does not exibit additional significant peak pressures. From these experiments, the generated pressures for impact velocities of 45 m/s and 16 m/s are measured to be respectively 4 MPa ± 1.5 and 1.5 ± 0.4 MPa with the hydrophone, while they are 2.5 MPa and 1.1 MPA ± 0.1 with the floating PVDF. Uncertainities obtained by the floating PVDF are less than the ones obtained with the hydrophone. In the observed period, there are only one positive peak and then moderated oscillations of pressure starting with a negative peak, which likely induced cavitation cloud as observed by the fast camera, their frequency matches with the one predicted by the Rayleigh-Plesset model describing the bubble dynamics. This cavitation cloud generates bubbles that mitigate the second peak of pressure observed on figure 6.Oscillations of a shorter period are attributed to be the reemission of compressive waves during the bubbles dynamics. In all the recorded pressure signals, it can be observed that the minimum negative pressure never goes below -1.2 MPa. The duration of the first peak of pressure remains more or less the same as the one on the first peak.

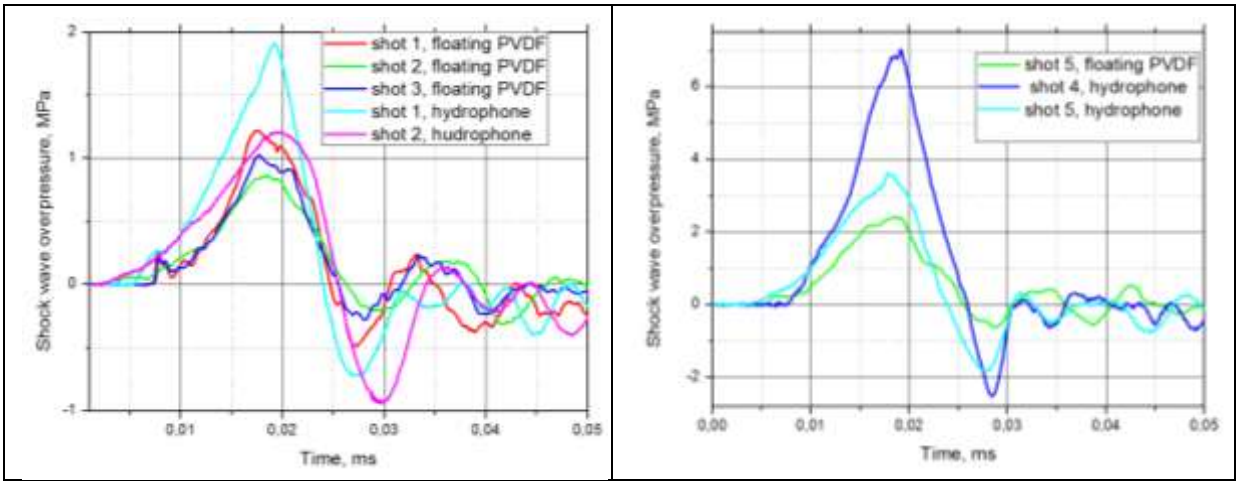

Figure 7.Shock wave overpressure comparison between floating PVDF and hydrophone measuremets

Pressure profiles presented in figure 7 a) are obtained with impact velocities presented in table 3.

The pressure profiles in time presented in figure 7 a) and b) do not evidence the arival time of the shock wave at the pressure sensore. The signals have been processed in the manner described by figure 7 in order to analyze the rising front coresponding to compressive waves and the decreasing profiles due to release waves or edge effects.

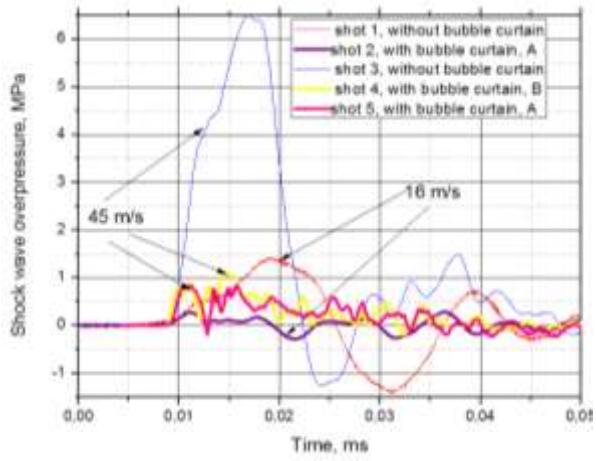

Figure 8.Bubble curtain mitigation capacity given by hydrophone measurement

In the presence of bubble curtain the pressure profile is significantly influenced by the interaction between the shock wave and the bubble curtain.

Table 5: Shock wave parameters obtained from hydrophone measuremets

Pressure load Bar	Terminal velocity m/s	Curtain	Pmax hydrophone (MPa)	Positive impulse MPa*ms
2	16	off	1.41	0.0133
2	15.7	A	0.19	0.00134
7	50.7	off	7.02	0.06
7	42	B	0.76	0.009
	51.5	A	1.37	0.01

Shock experiments were carried out with and without bubble curtain respectively with A and B bubble generators (respectively 6 L/min and 7 L/min) and the remaining pressure after the crossing of the bubble curtain has been measured about 10 cm after the curtain, 149 mm from the anvil (fig. 3).Without turning on the bubbling system (no curtain), a shot at 50.7 m/s leads to a peak of pressure of 7.02 MPa while a shot at 16 m/s lead to a peak pressure of 1.41 MPa. In presence of bubble curtain of type A with 6 L/min flowrate resulted in a peak pressure diminished from 1.41 MPa down to 0.19 MPa (86.5% attenuation) for an impact velocity of 15.7 m/s. The pressure decreased from 7.02 MPa down to 1.37 MPa for an impact velocity of abouot 51 m/s (83% attenuation) for pipe A and down to 0,76 MPa for an impact velocity 42 m/s for pipe B (table 5). Respective impulses are also strongly attenuated of more than 80% (table 6). Because of the difference between the impact velocities, it can not be estimated which type of pipes mitigates better the shock wave effects.

Table 6: Bubble curtain mitigation capacity

Impact vel m/s	Bubble generator	Impulse attenuation %	Pmax attenuation %
16 m/s	A	86.5	89
45 m/s	A	83	80
	B	85	89

6. Numerical simulation of underwater shock wave generation by projectile and target impact

Numerical simulations with the Finite Element Method in explicit scheme were performed in order to correlate experiments, by using ANSYS Autodyne®. In the numerical model, axis-ymmetrical geometry is considered. The projectile and the anvil are simulated as Lagrangian media and the water in the tank is considered Eulerian (fig. 9).

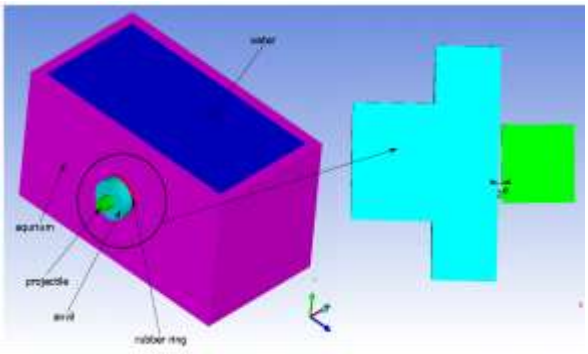

Figure 9.3D numerical configuration of underwater shock wave generation and propagation.

In AUTODYN, (2003), liquid media, projectile and anvil behavior are characterized by shock equation of state for the compression phase, as follows:

$$D = c_0 + su \quad (1)$$

where D is the shock wave, c_0 is the sound speed in the material, s is the shock characteristic of the material and u is the particle velocity behind the shock wave. The out of shock phase is described by the Mie-Grüneisen equation ofstate (2):

$$P(E,v) - P_0(v) = \frac{\Gamma}{v}(E - E_0(v)) \quad (2)$$

with v= 1/ρ masic volum; E is the internal energy and Γ(v) is Grüneisen coeficient depending on the material.

Table 7 shows the material characteristics that were used in the numerical model:

Table 7 : Material characteristics used in AUTODYN.

Material	ρ_0 (g/cm3)	C_0(m/s)	s	Γ_0
Water	0.998	1483	1.921	1.87
Anvil	2.81	5380	1.337	2.1
Projectile	2.78	5380	1.337	2.1

Johnson Cook flow stress model [Johnson, 1985] is used in order to characterize the viscoplastic behaviour of the projectile and anvil (3):

$$\sigma_y(\varepsilon_P, \dot{\varepsilon_P}, T) = [A + B(\varepsilon_P)^n]\left[1 + Cln\left(\dot{\varepsilon_P^*}\right)\right]$$

$$[1 - (T^*)^m] \quad (3)$$

where σ_y is the flow stress, ε_P is the plastic stain, $\dot{\varepsilon_P}$ plastic strain rate, A, B, C, m and n are material properties.

Table 8: Material properties for projectile and anvil

Material	A	B	C	m	n
AL projectile	2.65e5	4.26e5	0.015	1	0.34
Al anvil	2.65e5	3.02e5	0.015	1	0.46

A spallation model is implemented for water in order to avoid negative pressure waves propagation and be more representative of the cavitation process.

The numerical simulation has been conceived for several impact angles, respectively 2, 1 and 0.5 degrees.

During experimental trials, underwater shock wave overpressure has been recorded by means of three pressure sensors. Overpressure profile in time at the free interface of the anvil is given by the fixed PVDF. Firstly, we have analized the underwater compression wave parameters generated by the impact of a projectile at 45 m/s, given by the numerical simulation (fig. 10), for all impact angles.

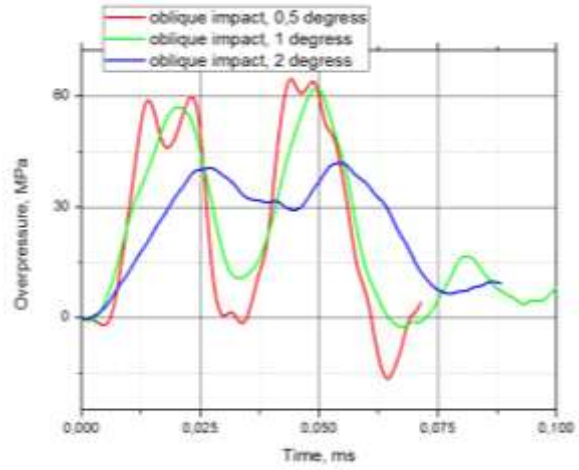

Figure 10.Velocity induced by shock wave to the anvil free face

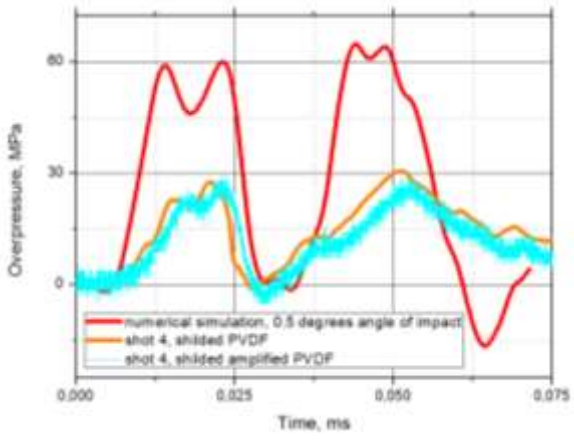

Figure 11.Comparison between experimental presssure profile and numerical results at the anvil free face.

A first conclusion that results directly from analyzing the overlap of pressure profiles, obtained after performing the numerical simulation, is that the impact angle has a major influence on shock wave generation and propagation into the anvil and further inside the water tank. The incident shock wave overpresure increases, as expected, with the decrease of the impact angle and also anvil lateral effects are more obvious for smaller angles.

The pressure computed for the smallest impact angle is then compared with the one measured by the PVDF sensor, like in figure 6 but for 45 m/s impact, at the anvil/water interface (fig.11).

The two pressure profiles, respectively numerical and experimental one, are characterized by a first double peak which differs aproximatly with 50% one from the other.

The PVDF gauge was shielded against electrostatic and electromagnetic parasites. The gauge was connected in current mode. Records were comparaed with the voltage signal given by a PVDF connected to a Kistler charge amplifier type 5011, with sensor sensitivity set at 15,4 pC/M.U and scale 50 M.U./V. Both current or charge amplified modes give similar results, except that the voltage scale of the oscilloscope was not really adapted in the case of the charge amplified record. It could be measured that the pressure transmitted into the water is around 30 MPa for the impact velocity of 45 m/s, while it was 8 MPa at 16 m/s. The numerical simulation here again gives over estimated signals that might be explained by air cushion phenomena that occur due to the flat front part of the projectile. The computed signal has a slow rising front after which it can be observed a double peack, as in the experimental data, being explained by the anvil lateral effects.

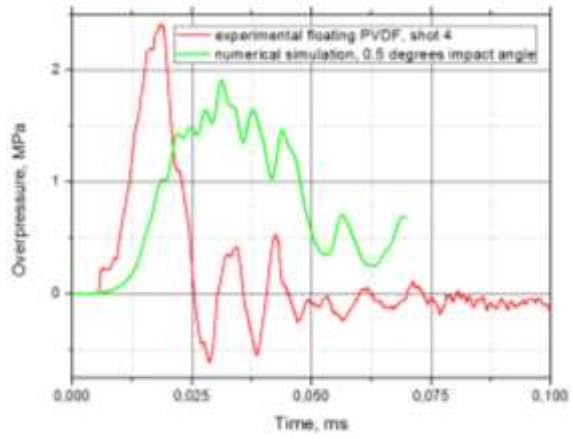

Figure 12.Comparison between experimental presssure profile and numerical results for floating PVDF.

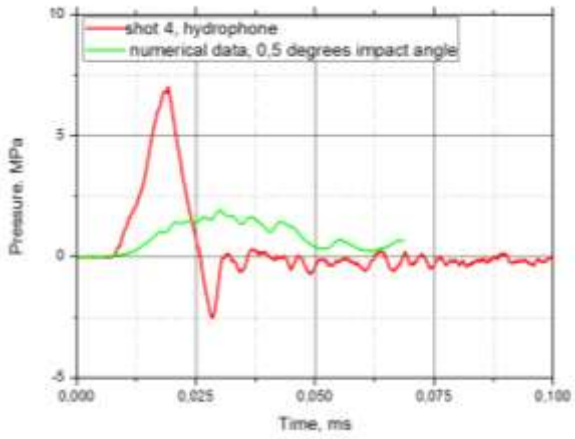

Figure 13.Comparison between experimental presssure profile and numerical results for hydrophone position.

The shock wave overpressure has been compared with numerical simulation also for the second PVDF sensor (hung in the water, on the path of the wave, it is abusively called floating PVDF), positioned as is described in figure 3. The comparison with numerical simulation has beed performed taking into consideration the incident shock wave and is represented in the fig. 12.

The computed pressure profile presents a maximu value which differs from the exprimental one with 20%. . The computed signal just falls and stays near zero level after the first peaks of pressure. It is due to the action of the damage model affected to the water in order to considere cavitation when the pressure goes down to zero. It can be seen that this criteria is exaggerated since in reality, negative pressure can be accepted as seen in experimental signal. In this case, cavitation does not act as a “cut off” but as a cloud of bubbles arroud which the waves can still pass, what explain the signal after the negative peak.

The first observation that results from the graph analyses is the discrepancies between the rising fronts corresponding to experimental and numerical profils. The possible phenomenon associated with this mismatches is the air cushion generated before the impact between the projectile and target (fig. 14).

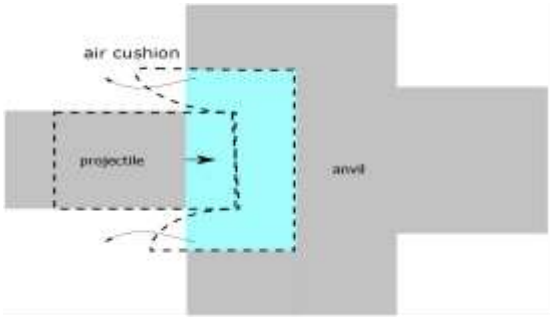

Figure 14.Air cushion phenomena due to flat cylindrical projectile impacting the anvil.

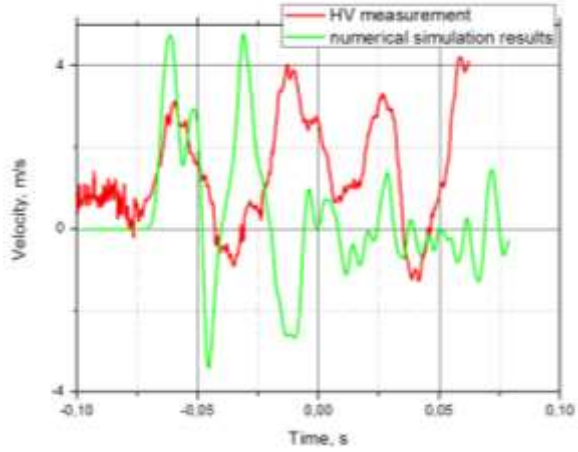

Figure 15.Anvil free face velocity comparison with experimental HV measurement

After the impact, the shock wave propagates through the target into the water tank and induces at the anvil interface a particle velocity which has been measured with the laser technique and compared with the numerical simulation like in figure 15. Once again, the numerical results are higher than the experimental one, being characterized by shorter phase duration.

7. Conclusions

In the present work it has been described an experimental procedure performed in order to characterize a bubbling pipe in laboratory conditions. Then, the mitigation capacity of a bubble curtain generated by blowing compressed air inside two different perforated pipes has been assessed with an experimental set-up at the laboratory scale. This set-up is able to generate blast-like compression wave but also multi peak pressure loading that give a longer impulse, more representative of pressure signal generated by pile driving in maritime works. The bubbling has been characterized by three different techniques as high speed camera recording, microphone and single optical probe and its main characteristics (bubble radius, flowrate, gas fraction) have been determined.

Shock wave overpressure has been analyzed using three pressure sensors, among them, PVDF sensors that have given valuable time resolved pressure records in water. Experimental results have been correlated with numerical simulation data with the observation that phenomena as air cushion has to be taken into consideration in future research regarding underwater pressure wave attenuation. The mitigation observed for bubble generator A (6 L/min flowrate, 10 mm hole spacing and 0.8 mm hole diameter) is about 89% in peak pressure and 86.5 % in impulse for 16 m/s impact velocity and 80% in peak pressure and 83% in impulse for 45 m/s impact velocity. The second bubble generator, (7 L/min flowrate, 12 mm hole spacing and 1.2 mm hole diameter) is characterized by a mitigation capacity about 85% in peack pressure and 89% in impulse.

8. Acknowledgements:

The author would like to thank ENSTA Bretagne, especially F. Montel and M. Legris, the Region Bretagne and the European Union for their financial supports. They also want to thank MTA and METRA from Bucharest for participating in this study.

References

[1] ANDO, Keita; COLONIUS, Tim; BRENNEN, Christopher E. Numerical simulation of shock propagation in a polydisperse bubbly liquid. International Journal of Multiphase Flow, 2011, 37.6: 596-608.

[2] BAUER, François. PVDF shock sensors: applications to polar materials and high explosives. Ultrasonics, Ferroelectrics, and Frequency Control, IEEE Transactions on, 2000, 47.6: 1448-1454.
[3] BULSON, P. S. The theory and design of bubble breakwaters. Coastal Engineering Proceedings, 1968, 1.11.
[4] CROCI, Kilian, et al. Mitigation of underwater explosion effects by bubble curtains: experiments and modelling. In: 23rd MABS (Military Aspects of Blast and Shock), Oxford, UK, 7-12 September 2014. 2014. p. 14 p.
[5] ESPINOSA, H. D.; LEE, S.; MOLDOVAN, N. A novel fluid structure interaction experiment to investigate deformation of structural elements subjected to impulsive loading. Experimental Mechanics, 2006, 46.6: 805-824.
[6] GRAFF, Karl F. Wave motion in elastic solids. Courier Corporation, 1975.
[7] GRANDJEAN, Hervé; JACQUES, Nicolas; ZALESKI, Stéphane. Shock propagation in liquids containing bubbly clusters: a continuum approach. Journal of Fluid Mechanics, 2012, 701: 304-332.
[8] HAWASS, Ahmed; MOSTAFA, Hosam; ELBEIH, Ahmed. Multi-layer protective armour for underwater shock wave mitigation. Defence Technology, 2015, 11.4: 338-343.
[9] JOHNSON, Gordon R.; COOK, William H. A constitutive model and data for metals subjected to large strains, high strain rates and high temperatures. In: Proceedings of the 7th International Symposium on Ballistics. 1983. p. 541-547.
[10] KAMEDA, Masaharu, et al. Shock waves in a uniform bubbly flow. Physics of Fluids (1994-present), 1998, 10.10: 2661-2668.
[11] KOSCHINSKI, S.; KOCK, K. H. Underwater unexploded ordnance–methods for a cetacean-friendly removal of explosives as alternatives to blasting. International Whaling Commission. Scientific Committee Paper SC/61 E, 2009, 21.
[12] LA PRAIRIE, Method of blasting, US 2699117 A, 1950;
[13] LATOURTE, Felix, et al. Failure mechanisms in composite panels subjected to underwater impulsive loads. Journal of the Mechanics and Physics of Solids, 2011, 59.8: 1623-1646.
[14] LEGENDRE D., ZENIT R., VELEZ-CORDERO R., On the deformation of gas bubbles in liquids, Physics of Fluids, American Institute of Physics, 2012, vol. 24, ISSN 1070-6631;
[15] MALLOCK, A. The damping of sound by frothy liquids. Proceedings of the Royal Society of London. Series A, Containing Papers of a Mathematical and Physical Character, 1910, 84.572: 391-395.
[16] MOORE, D. W. The rise of a gas bubble in a viscous liquid. Journal of Fluid Mechanics, 1959, 6.01: 113-130.
[17] RAMAKRISHNAN, S., KUMAR, R. and KULOOR R., Studies in bubble formation-I Bubble formation under constant flow conditions, Chemical Engineering Science, 1969, 24.4:731-747.
[18] SAITO, T., et al. Experimental and numerical studies of underwater shock wave attenuation. Shock Waves, 2003, 13.2: 139-148.
[19] SATYANARAYAN, A.; KUMAR, R.; KULOOR, N. R. Studies in bubble formation—II bubble formation under constant pressure conditions. Chemical Engineering Science, 1969, 24.4: 749-761.
[20] SLABBEKOORN, Hans, et al. A noisy spring: the impact of globally rising underwater sound levels on fish. Trends in Ecology & Evolution, 2010, 25.7: 419-427.
[21] STRAND, O. T., et al. Compact system for high-speed velocimetry using heterodyne techniques. Review of Scientific Instruments, 2006, 77.8: 083108.
[22] SUROV, V. S. Interaction of a shock wave with a bubble screen. Technical physics, 1999, 44.1: 37-43.
[23] XIE, Shuyi; TAN, Reginald BH. Bubble formation at multiple orifices—bubbling synchronicity and frequency. Chemical engineering science, 2003, 58.20: 4639-4647.